Stem Cell Reports, Volume *10*

Supplemental Information

Generation of TCR-Expressing Innate Lymphoid-like Helper Cells that Induce Cytotoxic T Cell-Mediated Anti-leukemic Cell Response

Norihiro Ueda, Yasushi Uemura, Rong Zhang, Shuichi Kitayama, Shoichi Iriguchi, Yohei Kawai, Yutaka Yasui, Minako Tatsumi, Tatsuki Ueda, Tian-Yi Liu, Yasutaka Mizoro, Chihiro Okada, Akira Watanabe, Mahito Nakanishi, Satoru Senju, Yasuharu Nishimura, Kiyotaka Kuzushima, Hitoshi Kiyoi, Tomoki Naoe, and Shin Kaneko

Supplemental Information

Supplemental method

Cells

We isolated peripheral blood mononuclear cells (PBMCs) from healthy donors as described.(Liu et al., 2008) Human monocyte-derived-DCs were induced as described.(Uemura et al., 2009) Human CML cell line K562, human myelogenous leukemia cell line THP-1, and human lung-cancer cell line PC9 were purchased. Mouse L-fibroblasts transfected with HLA class II genes were used as described.(Tabata et al., 1998) For cells isolated from healthy adults, informed consent about their use was obtained from all donors. The entire study was conducted in accordance with the Declaration of Helsinki and with the approval of the appropriate institutional ethics boards.

Transfectants

cDNA encoding *HLA-DR9 (DRB1*09:01)* was previously described.(Ueda et al., 2016) cDNA encoding *BCR-ABL p210* was purchased from Addgene (Cambridge, MA,

USA).(He et al., 2002) cDNA encoding *BCR-ABL p210*, *HLA-A24 (A*24:02)*, *HLA-DRA*, or *HLA-DR9*, or minigene encoding HLA-A24-restricted modified $WT1_{235–243}$ epitope was inserted into lentiviral vector CSII-EF-MCS (RIKEN BioResource Center, Tsukuba, Japan). Lentivirus transduction was performed as described.(Zhang et al., 2015) K562-expressing luciferase gene (K562-Luc) was transduced with lentivirus vectors to express *HLA-A*24:02* and minigene encoding modified $WT1_{235–243}$ epitope (K562-Luc-A24-WT1 minigene). THP-1 was transduced with lentivirus vectors to express *HLA-DRA*01:01* and *HLA-DRB1*09:01* and/or *BCR-ABL p200* (THP-1-DR9, THP1-DR9-BCRABL).

Flow cytometry and antibodies used for functional assays

The monoclonal antibodies (mAbs) used for flow cytometry and functional assays are listed in Table S1. HLA-A*24:02/$WT1_{235-243}$ tetramer was used to detect WT1 peptide-specific CTLs, with HLA-A*24:02/HIV $Env_{584-592}$ tetramer serving as a negative control. The stained cell samples were analyzed using FACSCalibur and FACSAria II flow cytometer (BD Biosciences), and the data were processed using

FlowJo software (Tree Star, Ashland, OR, USA). Relative fluorescence intensity (RFI) was calculated as the ratio of the mean fluorescence intensity (MFI) of specific markers to the MFI of isotype controls.

RNA Sequencing

cDNA was synthesized using a SMARTer Ultra Low Input RNA and sequenced with Illumina Sequencing-HV kit (Clontech, Mountain View, CA, USA), after which the Illumina library was prepared using Low Input Library Prep kit (Clontech). The libraries were sequenced using HiSeq 2500 in 101 cycle Single-Read mode. All sequence reads were extracted in FASTQ format using BCL2FASTQ Conversion Software 1.8.4 in the CASAVA 1.8.2 pipeline. The sequence reads were mapped to hg19 reference genome, downloaded on December 10, 2012, using TopHat v2.0.8b, and quantified using RPKMforGenes. The data have been deposited in NCBI Gene Expression Omnibus (http://www.ncbi.nlm.nih.gov/geo/, accession number GSE94332). Subpopulations from iPS-T cells were obtained on the basis of CD161 and c-Kit expression (Figure S2C), and their gene expression profiles were compared to NK cells,

ILC1s, ILC2s, ILC3s, αβ T cells, and γδ T cells. NK cells, ILC1s, ILC2s, ILC3s, αβ T cells, and γδ T cells were separated from PBMCs of healthy donors (Figure S2D). For pathway analysis, differentially expressed genes were defined by calculating the fold-change of the averaged expression ($|\log2FC| \geq 1$). Hypergeometric tests were conducted using org.Hs.eg.db 3.2.3 of R3.2.2 with GOstats 2.36.0 along with the annotation packages of GO.db 3.2.2 (Gene Ontology analysis) and KEGGprofile 1.12.0 along with the annotation packages of KEGG.db 3.2.2 (KEGG pathway analysis).

Analysis of T cell antigen receptor (TCR) gene rearrangement of T cell clone

The *V*, *D*, and *J* segments of the rearranged TCR-α and TCR-β chains of T cells or iPS-T cells were identified as described.(Uemura et al., 2003) The gene-segment nomenclature used follows the ImMunoGeneTics (IMGT) usage; the *V*, *D*, and *J* segments were identified by comparing the resulting sequences against the IMGT database (http://www.imgt.org/) with an online tool (IMGT/V-QUEST).

Real-time PCR

Total RNA was extracted from iPSCs using an RNeasy Micro kit (Qiagen, Valencia, CA). cDNA was synthesized using High Capacity cDNA Reverse Transcription kits (Applied Biosystems, Foster City, CA, USA) with random 6-mer primers, followed by RT-PCR using ExTaq HS (Takara, Shiga, Japan) and by quantitative-PCR using a TaqMan Array Human Stem Cell Pluripotency Card (Applied Biosystems). Individual PCR reactions were normalized against 18S rRNA.

In vivo bioluminescence imaging

Tumor-bearing mice were injected with 200 μl D-Luciferin (15 mg/ml, VivoGlo Luciferin; Promega, Madison, WI, USA) under 2% inhaled isoflurane anesthesia, and bioluminescent images were obtained using IVIS Lumina II with Living Image Software 3.2 (Xenogen, Alameda, CA, USA).

REFERENCES

He, Y., Wertheim, J.A., Xu, L., Miller, J.P., Karnell, F.G., Choi, J.K., Ren, R., and Pear, W.S. (2002). The coiled-coil domain and Tyr177 of bcr are required

to induce a murine chronic myelogenous leukemia-like disease by bcr/abl. Blood *99*, 2957-2968.

Liu, T.Y., Uemura, Y., Suzuki, M., Narita, Y., Hirata, S., Ohyama, H., Ishihara, O., and Matsushita, S. (2008). Distinct subsets of human invariant NKT cells differentially regulate T helper responses via dendritic cells. European journal of immunology *38*, 1012-1023.

Tabata, H., Kanai, T., Yoshizumi, H., Nishiyama, S., Fujimoto, S., Matsuda, I., Yasukawa, M., Matsushita, S., and Nishimura, Y. (1998). Characterization of self-glutamic acid decarboxylase 65-reactive CD4+ T-cell clones established from Japanese patients with insulin-dependent diabetes mellitus. Human immunology *59*, 549-560.

Ueda, N., Zhang, R., Tatsumi, M., Liu, T.Y., Kitayama, S., Yasui, Y., Sugai, S., Iwama, T., Senju, S., Okada, S.*, et al.* (2016). BCR-ABL-specific CD4+ T-helper cells promote the priming of antigen-specific cytotoxic T cells via dendritic cells. Cell Mol Immunol.

Uemura, Y., Liu, T.Y., Narita, Y., Suzuki, M., Nakatsuka, R., Araki, T., Matsumoto, M., Iwai, L.K., Hirosawa, N., Matsuoka, Y.*, et al.* (2009). Cytokine-dependent modification of IL-12p70 and IL-23 balance in dendritic cells by ligand activation of Valpha24 invariant NKT cells. Journal of immunology *183*, 201-208.

Uemura, Y., Senju, S., Maenaka, K., Iwai, L.K., Fujii, S., Tabata, H., Tsukamoto, H., Hirata, S., Chen, Y.Z., and Nishimura, Y. (2003). Systematic analysis of the combinatorial nature of epitopes recognized by TCR leads to identification of mimicry epitopes for glutamic acid decarboxylase 65-specific TCRs. Journal of immunology *170*, 947-960.

Zhang, R., Liu, T., Senju, S., Haruta, M., Hirosawa, N., Suzuki, M., Tatsumi, M., Ueda, N., Maki, H., Nakatsuka, R.*, et al.* (2015). Generation of mouse pluripotent stem cell-derived proliferating myeloid cells as an unlimited source of functional antigen-presenting cells. Cancer immunology research.

Figure S1

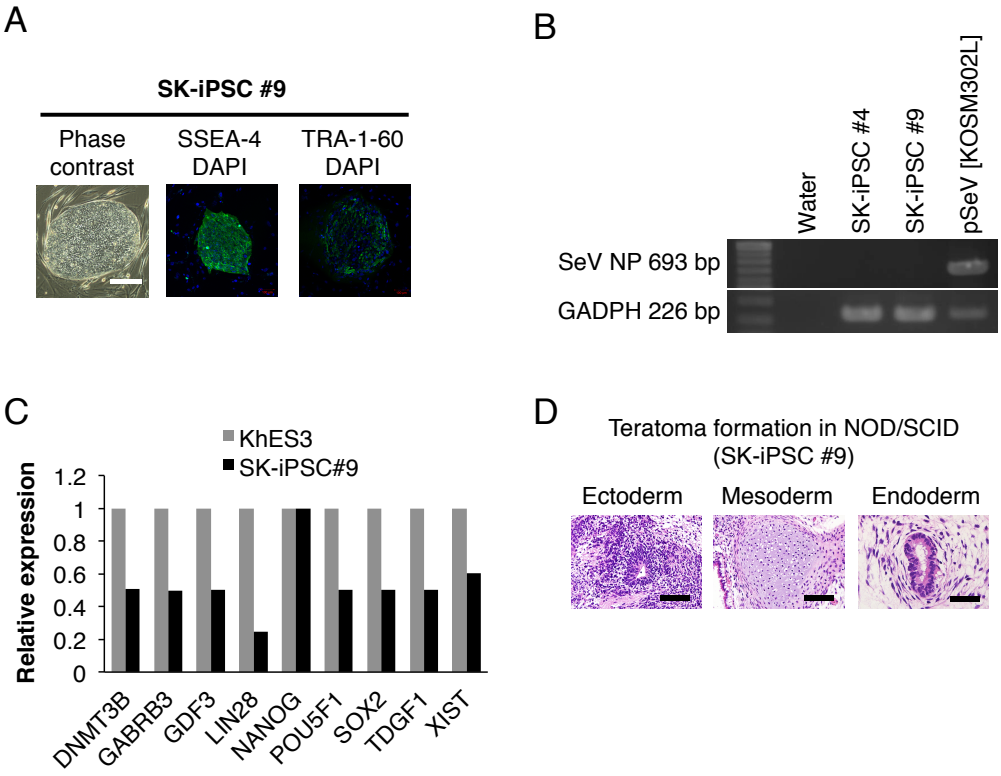

E

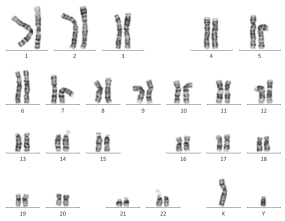

SK-iPSC #9
46XY (20/20)

Figure S2

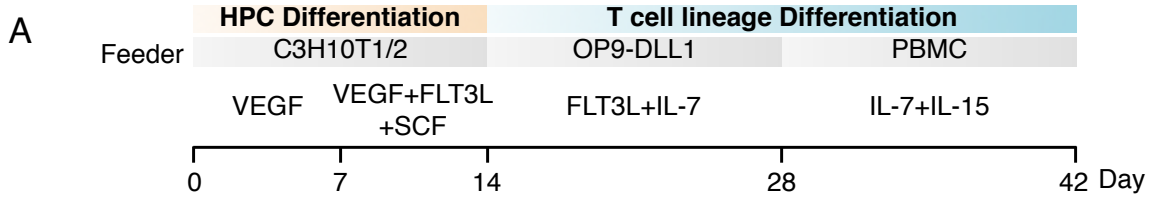

B

SK, Original Th1 Clone

TCRV	FW	CDR3	FW	TCRJ	CDR3 length
*TRAV29/DV5*01*	CAA	SLPQGGSEKL	VFG	*TRAJ57*01*	10
*TRBV2*01*	CAS	SDQGGDNEQ	FFG	*TRBJ2-1*01*	9

iPS-T

TCRV	FW	CDR3	FW	TCRJ	CDR3 length
*TRAV29/DV5*01*	CAA	SLPQGGSEKL	VFG	*TRAJ57*01*	10
*TRBV2*01*	CAS	SDQGGDNEQ	FFG	*TRBJ2-1*01*	9

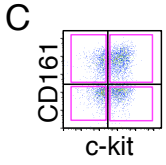

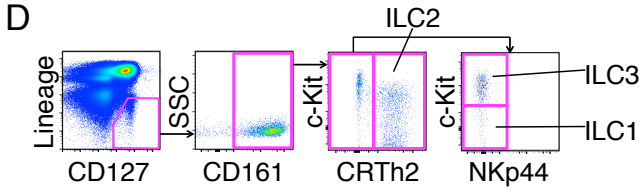

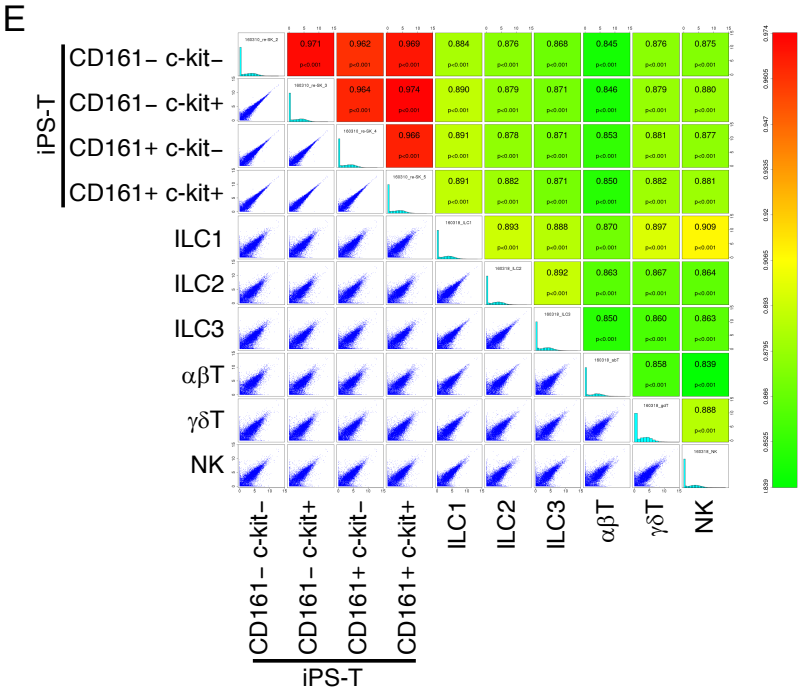

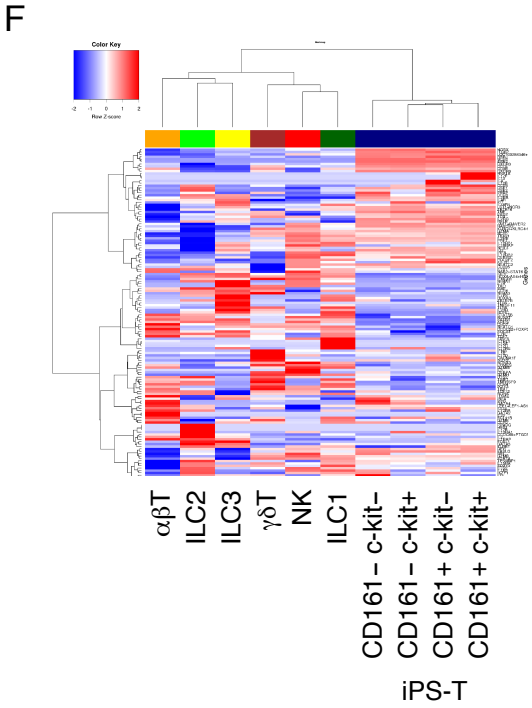

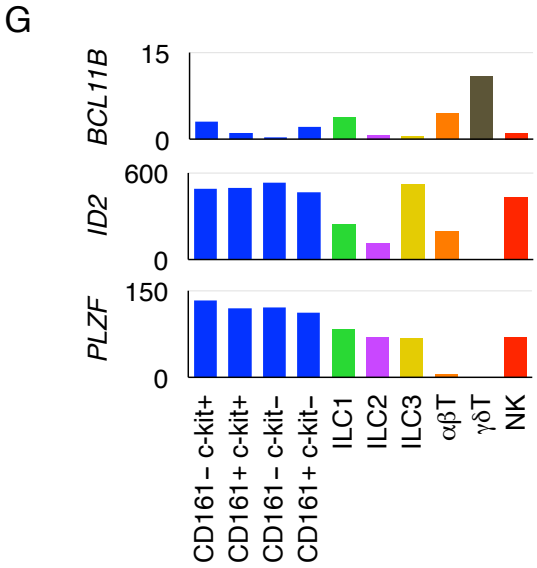

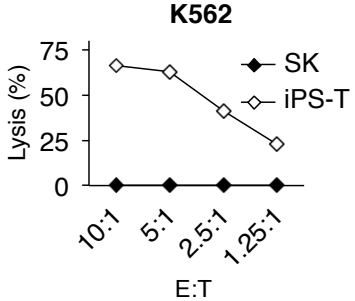

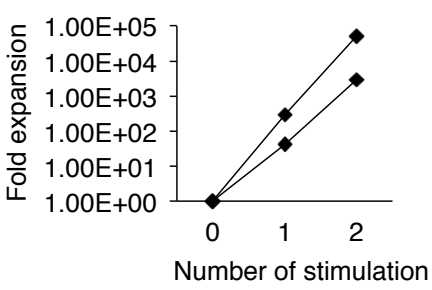

Figure S3

A

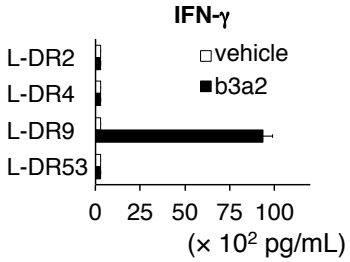

B

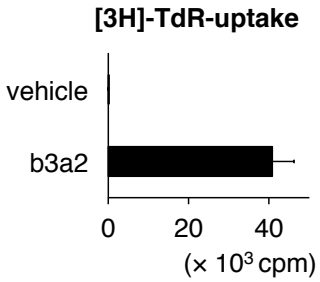

C

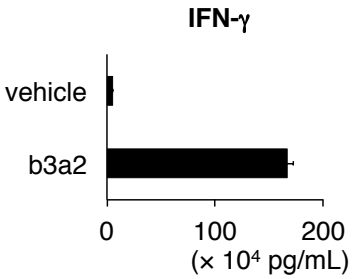

D

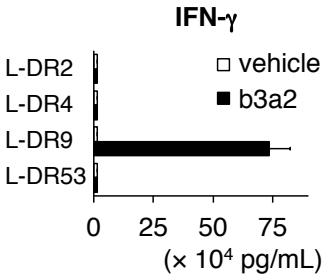

E

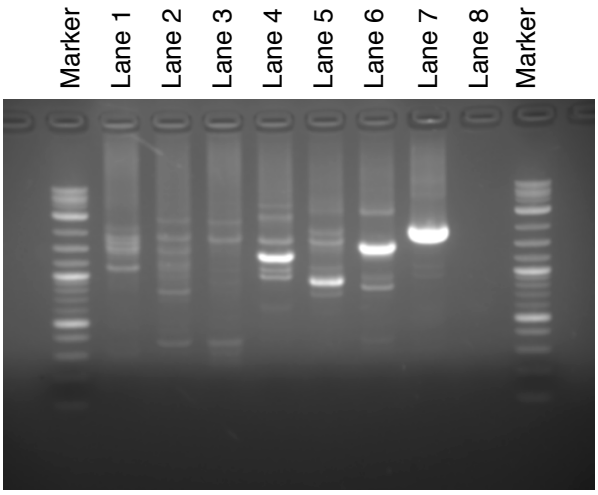

Lane 1: SK CD4+ iPS-T cell Library 1 (DraI digested)
Lane 2: SK CD4+ iPS-T cell Library 2 (SspI digested)
Lane 3: SK CD4+ iPS-T cell Library 3 (HpaI digested)
Lane 4: Retrovirus integrated iPSC clone,TkT3V1-7 Library 1 (DraI digested)
Lane 5: Retrovirus integrated iPSC clone,TkT3V1-7 Library 2 (SspI digested)
Lane 6: Retrovirus integrated iPSC clone,TkT3V1-7 Library 3 (HpaI digested)
Lane 7: Positive control (contained in the kit)
Lane 8: Negative control (H2O)

Figure S4

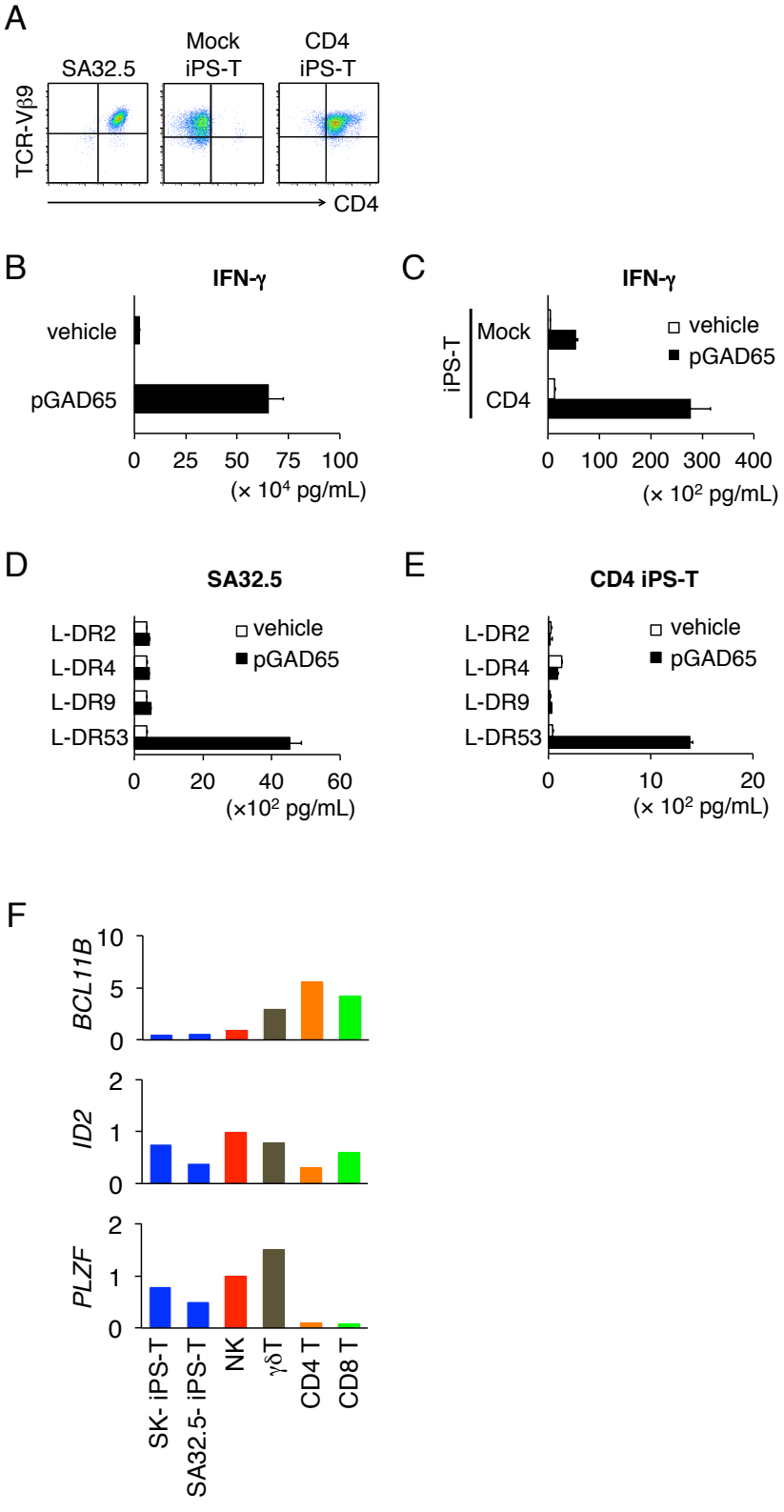
A
SA32.5
Mock iPS-T
CD4 iPS-T
TCR-Vβ9
CD4
B
IFN-γ
vehicle
pGAD65
0 25 50 75 100
(× 10⁴ pg/mL)
C
IFN-γ
iPS-T
Mock
CD4
vehicle
pGAD65
0 100 200 300 400
(× 10² pg/mL)
D
SA32.5
L-DR2
L-DR4
L-DR9
L-DR53
vehicle
pGAD65
0 20 40 60
(×10² pg/mL)
E
CD4 iPS-T
L-DR2
L-DR4
L-DR9
L-DR53
vehicle
pGAD65
0 10 20
(× 10² pg/mL)
F
BCL11B
ID2
PLZF
SK- iPS-T
SA32.5- iPS-T
NK
γδT
CD4 T
CD8 T

Figure S5

A

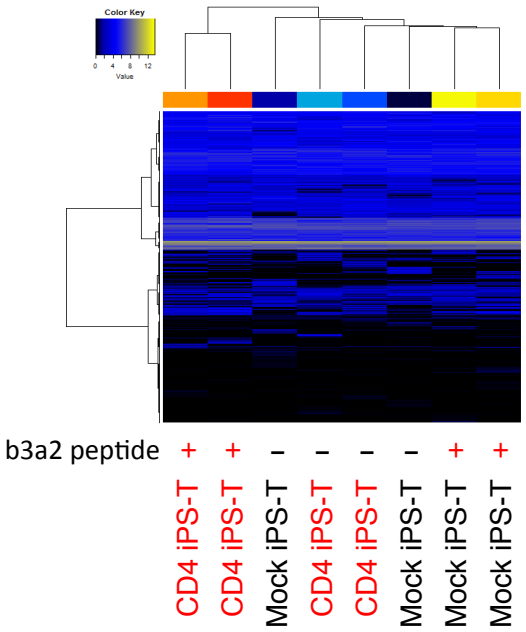

B

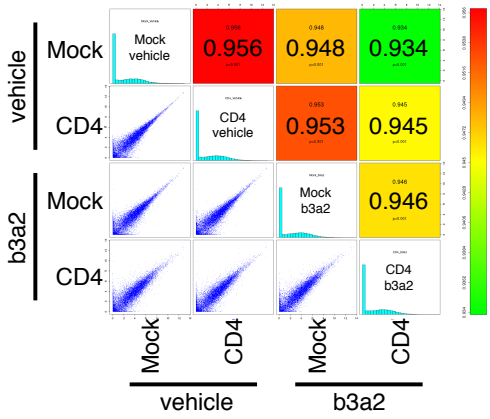

C

GO term	*p* value
Cell proliferation-related gene ontology	
Mitosis	5.47E-14
Nuclear division	5.47E-14
M phase of mitotic cell cycle	8.54E-14
Cell cycle phase	1.4E-13
Organelle fission	1.47E-13
Cell cycle process	2.31E-13
Mitotic cell cycle	7.85E-13

D

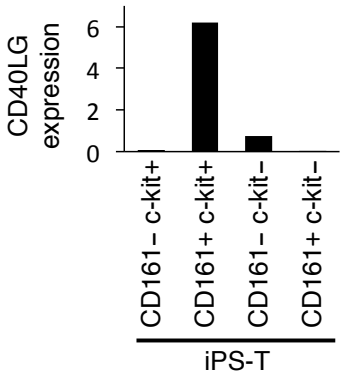

Figure S6

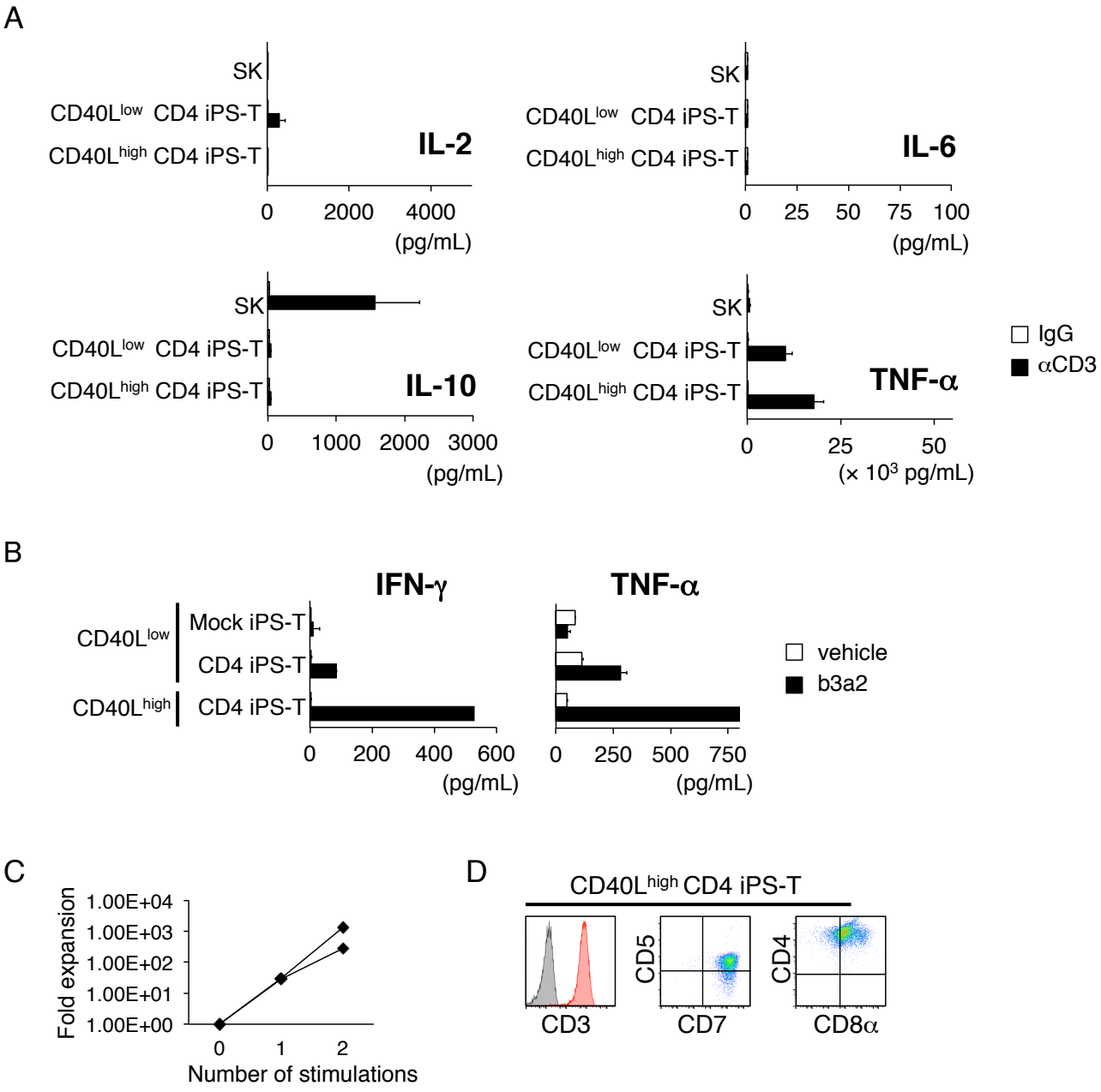
A
SK
CD40L^low CD4 iPS-T
CD40L^high CD4 iPS-T
IL-2
0 2000 4000
(pg/mL)
IL-6
0 25 50 75 100
(pg/mL)
IL-10
0 1000 2000 3000
(pg/mL)
TNF-α
0 25 50
(× 10^3 pg/mL)
IgG
αCD3
B
IFN-γ
TNF-α
CD40L^low
Mock iPS-T
CD4 iPS-T
CD40L^high
CD4 iPS-T
0 200 400 600
(pg/mL)
0 250 500 750
(pg/mL)
vehicle
b3a2
C
Fold expansion
1.00E+04
1.00E+03
1.00E+02
1.00E+01
1.00E+00
0 1 2
Number of stimulations
D
CD40L^high CD4 iPS-T
CD3
CD5
CD7
CD4
CD8α

Figure S7

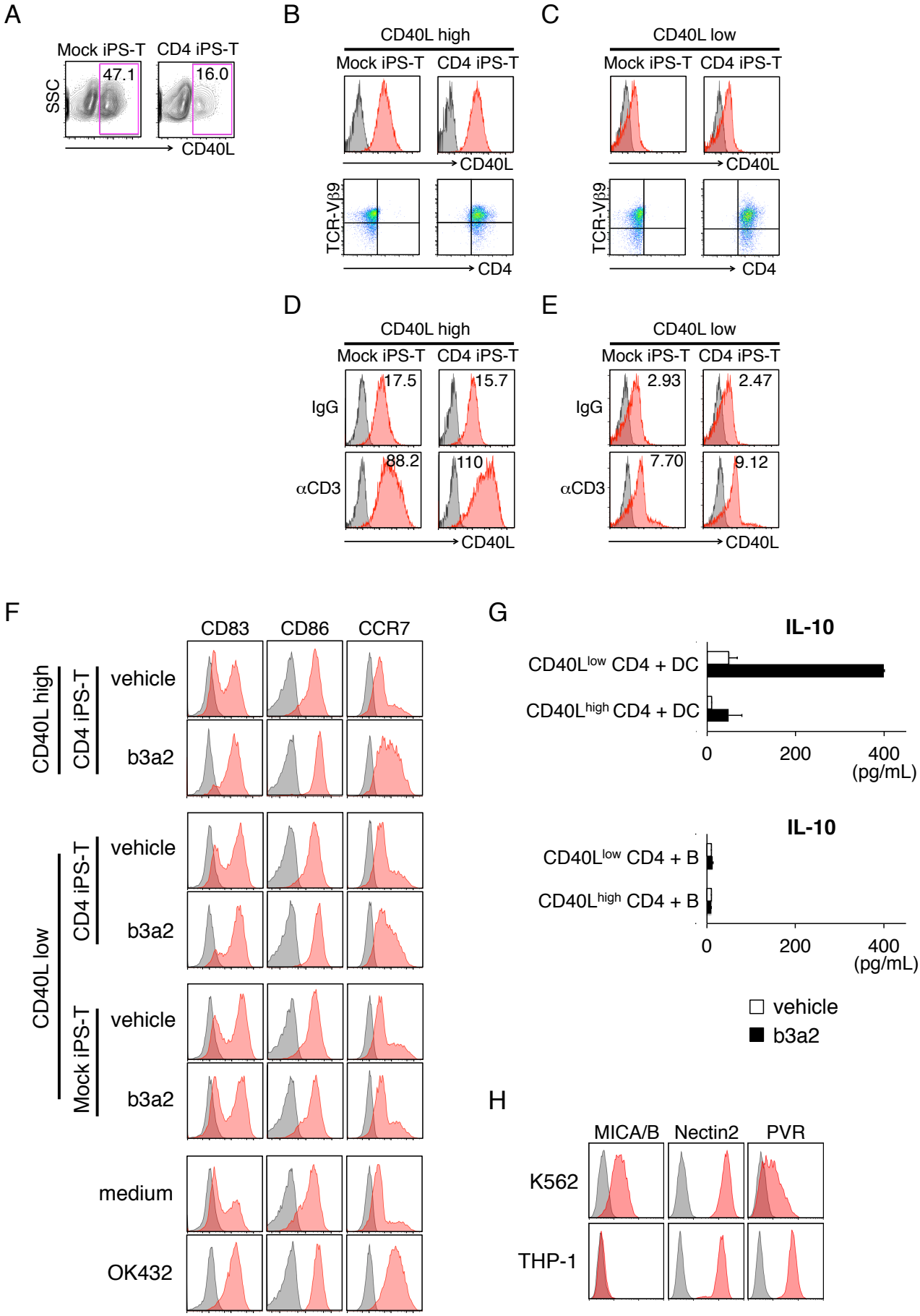
A
Mock iPS-T
CD4 iPS-T
47.1
16.0
SSC
CD40L
B
CD40L high
Mock iPS-T
CD4 iPS-T
CD40L
TCR-Vβ9
CD4
C
CD40L low
Mock iPS-T
CD4 iPS-T
CD40L
TCR-Vβ9
CD4
D
CD40L high
Mock iPS-T
CD4 iPS-T
IgG
17.5
15.7
αCD3
88.2
110
CD40L
E
CD40L low
Mock iPS-T
CD4 iPS-T
IgG
2.93
2.47
αCD3
7.70
9.12
CD40L
F
CD83
CD86
CCR7
CD40L high
CD4 iPS-T
vehicle
b3a2
CD40L low
CD4 iPS-T
vehicle
b3a2
Mock iPS-T
vehicle
b3a2
medium
OK432
G
IL-10
CD40L^low CD4 + DC
CD40L^high CD4 + DC
0
200
400
(pg/mL)
IL-10
CD40L^low CD4 + B
CD40L^high CD4 + B
0
200
400
(pg/mL)
vehicle
b3a2
H
MICA/B
Nectin2
PVR
K562
THP-1

Figure S8

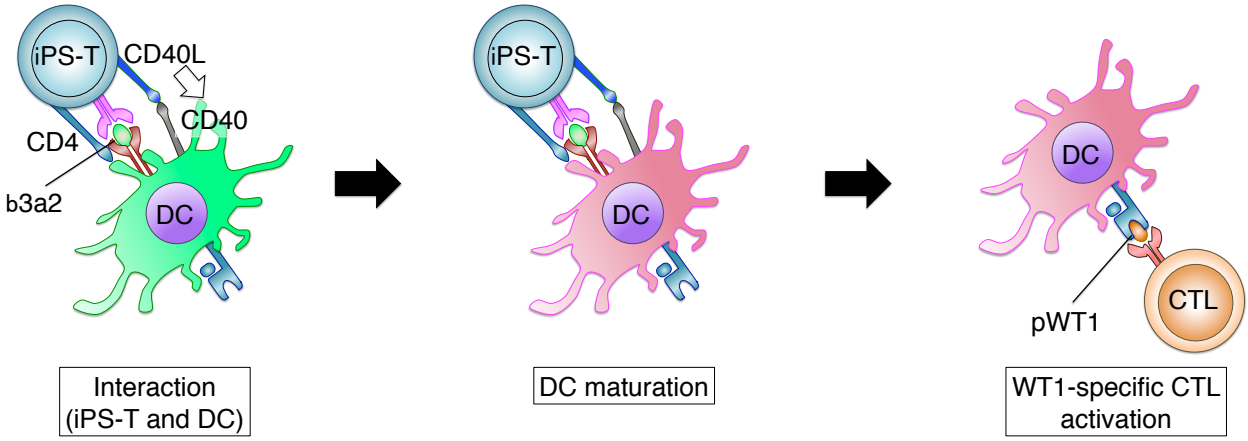
iPS-T
CD40L
CD40
CD4
b3a2
DC
iPS-T
DC
DC
CTL
pWT1
Interaction
(iPS-T and DC)
DC maturation
WT1-specific CTL
activation

Figure S1

Generation of iPSCs from b3a2-specific CD4$^+$ Th1 clone, related to materials and methods

(A) iPSC colonies derived from b3a2-specific CD4$^+$ Th1 clone (SK). Shown are representative phase contrast and immunofluorescent images. Scale bar represents 100 μm. **(B)** PCR-based analysis for detection of SeVdp genomic RNA remnants. Established iPSC colonies from the original CD4$^+$ Th1 clone (SK) (SK-iPSC) did not retain remnant SeVdp (KOSM) 302L vector. **(C)** Quantitative PCR analysis of pluripotency-related genes in SK-iPSCs. Individual PCR results were normalized to 18S ribosomal RNA levels (rRNA). Relative expression values to an embryonic stem cell line (KhES3) are indicated. **(D)** Representative HE-stained sections of a SK-iPSC-derived teratoma from an NOD/ShiJic-scid mouse. iPSCs differentiated into cell lineages derived from endoderm, mesoderm, and ectoderm. Scale bars represent 500 μm. **(E)** Representative karyotype analysis of SK-iPSCs.

Figure S2

Characteristics of T-lineage cells from CD4$^+$ Th1 clone-derived iPSCs, related to Figure 1

(A) Culture protocol for re-differentiation of T-lineage cells from CD4$^+$ Th clone-derived iPSCs. **(B)** TCR gene usage and *V*-(*D*)-*J* junction region sequences of the original CD4$^+$ Th1 clone (SK) and iPS-T cells. **(C)** CD161 and c-Kit expression profiles on iPS-T cells. **(D)** Representative flow cytometry profile of ILC subpopulations from PBMCs of healthy donors. ILC1s, ILC2s, and ILC3s were defined by expression of the indicated molecules. The lineage cocktail contained antibodies for CD1a, CD3, CD11c, CD14, CD19, CD34, CD94, CD123, BDCA2, FcεR1, TCRαβ, and TCRγδ. **(E)** Scatter plots representing the expression of each gene in the indicated pairs of cell types. Numbers in the panels denote pair-wise Pearson's correlation scores. **(F)** Two-way clustering of 146 selected gene expression profiles related to T cell/ILC differentiation and function (Table S3). **(G)** *BCL11B*, *ID2*, and *PLZF* expression in the indicated population. mRNA expression levels were determined by RNA-seq. **(E–G)** Subpopulations from iPS-T cells separated based on CD161 and c-Kit expression shown in (**C**) were compared to NK cells, ILC1s, ILC2s, ILC3s, αβ T cells, and γδ T

cells. **(H)** Cytotoxic activities of original $CD4^+$ Th1 clone (SK) and iPS-T cells to K562 cells. Cytotoxicity was measured by ^{51}Cr-release assay for 4 h at the indicated effector/target (E:T) ratios. Data are representative of two independent triplicate experiments. **(I)** Expansion of iPS-T cells. iPS-T cells were stimulated by PHA-P in the presence of PBMCs at 14-day intervals. Shown are representative results from two independent experiments.

Figure S3

HLA-DR9-restricted, b3a2 peptide-specific response of original $CD4^+$ Th1 clone, related to Figure 1

(A) HLA-DR–restricted IFN-γ production by $CD4^+$ iPS-T cells. $CD4^+$ iPS-T cells (5×10^4) were co-cultured with irradiated L-cell transfectants expressing the indicated HLA-DR (4×10^4) prepulsed with b3a2 peptide (10 μM). **(B)** Proliferative response of the original $CD4^+$ Th1 clone (SK) to antigenic peptide. T cells were co-cultured with autologous PBMCs in the presence of b3a2 peptide (10 μM). Proliferation was determined by the [^{3}H]-thymidine incorporation assay. Data shown are the means ± SD

and are representative of two independent triplicate experiments. **(C)** b3a2 peptide-specific IFN-γ production by the original $CD4^+$ Th1 clone. The original $CD4^+$ Th1 clone (1×10^5) was co-cultured with autologous DCs (5×10^4) that had been prepulsed with the b3a2 peptide (10 μM). **(D)** HLA-DR-restricted IFN-γ production by the original $CD4^+$ Th1 clone. The original $CD4^+$ Th1 clone (5×10^4) was co-cultured with irradiated L-cell transfectants (4×10^4) prepulsed with b3a2 peptide (10 μM). **(A, C, D)** IFN-γ level in the culture supernatant (24 h) was measured by ELISA. Data shown are the means ± SD of triplicate cultures and are representative of two independent experiments. **(E)** Retroviral integration site analysis of $CD4^+$ iPS-T cells by LAM-PCR. Retrovirus-integrated iPSC clone, TkT3V1-7, served as a positive control.

Figure S4

CD4 modification induces HLA class II-restricted responses in iPS-T cells derived from GAD65 peptide-specific $CD4^+$ Th clone, related to Figure 1

(A) Representative flow cytometry profiles of the indicated molecules on GAD65 peptide-specific $CD4^+$ Th clone (SA32.5) and iPS-T cells from SA32.5-derived iPSCs

transduced with Mock or CD4 gene. **(B)** GAD65 peptide-specific IFN-γ production by SA32.5. **(C)** GAD65 peptide-specific IFN-γ production by mock iPS-T cells and $CD4^+$ iPS-T cells, both from SA32.5-derived iPSCs. **(B, C)** IFN-γ level in the culture supernatant was measured by ELISA. SA32.5, mock iPS-T cells, or $CD4^+$ iPS-T cells (1×10^5) were co-cultured for 24 h with HLA-DR53 positive DCs (5×10^4) that had been prepulsed with GAD65 peptide (10 μM). Data shown are the means ± SD and are representative of two independent triplicate experiments. **(D)** HLA-DR-restricted IFN-γ production by SA32.5. **(E)** HLA-DR-restricted IFN-γ production by $CD4^+$ iPS-T cells from SA32.5-derived iPSCs. **(D, E)** IFN-γ level in the culture supernatant (24 h) was measured by ELISA. SA32.5 or $CD4^+$ iPS-T cells (5×10^4) were co-cultured with irradiated L-cell transfectants (4×10^4) that had been prepulsed with GAD65 peptide (10 μM). Data shown are the means ± SD of triplicate cultures and are representative of two independent experiments. **(F)** Measurement of *BCL11B*, *ID2*, and *PLZF* mRNA expression by real-time RT-PCR in the indicated population. Expression of each mRNA was normalized to that of *ACTB* mRNA (SK-iPS-T: iPS-T cells derived from b3a2-specific $CD4^+$ Th1 clone (SK), SA32.5-iPS-T: iPS-T cells derived from GAD65

peptide-specific $CD4^+$ Th clone (SA32.5)).

Figure S5

Gene expression of CD4 modified iPS-T cells, related to Figure 1

(A) Two-way clustering showing global gene expression profiles. Mock iPS-T cells and $CD4^+$ iPS-T cells were stimulated with vehicle or b3a2 peptide. THP-1-expressing HLA-DR9 was used as APCs. **(B)** Scatter plots representing the expression of each gene in the indicated pairs of cell types. Numbers in the panels denote pair-wise Pearson's correlation scores. **(C)** Gene ontology (GO) term enriched in genes significantly up-regulated in b3a2-stimulated $CD4^+$ iPS-T cells compared to in b3a2-stimulated Mock iPS-T cells. **(A–C)** Mock iPS-T cells and $CD4^+$ iPS-T cells were stimulated with vehicle or b3a2 peptide. THP-1-expressing HLA-DR9 were used as APCs. **(D)** CD40L gene expression of subpopulations from iPS-T cells. mRNA expression levels were determined by RNA-seq.

Figure S6

Function and surface phenotype of CD40L^{high} population from CD4^{+} iPS-T cells, related to Figure 2

(A) Cytokine production by the indicated populations. Each population was stimulated with plate-bound control IgG or anti-CD3 mAb (10 μg/mL). The original CD4^{+} Th1 clone (SK) served as a control. **(B)** Cytokine production by the indicated populations. Each population (1×10^4) was co-cultured with autologous DCs (2.5×10^4) that had been prepulsed with b3a2 peptide (10 μM). **(A–B)** Cytokine levels in the culture supernatant (24 h) were measured in a bead-based multiplex immunoassay. Data shown are the means ± SD of triplicate cultures and are representative of two independent experiments. **(C)** Expansion of CD40L^{high} CD4^{+} iPS-T cells. CD40L^{high} CD4^{+} iPS-T cells were stimulated with PHA-P in the presence of PBMCs at 14-day intervals. Shown are representative results of two independent experiments. **(D)** Representative flow cytometry profiles of the indicated molecules on CD40L^{high} and CD40L^{low} CD4^{+} iPS-T cells. Indicated surface molecules (red) and isotype-matched controls (gray) are shown.

Figure S7

CD40L^{high} CD4^{+} iPS-T cells derived from SA32.5-iPSCs, related to Figure 2-4

(A) Representative flow cytometry profiles of the indicated molecules on the indicated iPS-T cells from SA32.5-iPSCs on day 13 after PHA-P stimulation. The number of CD40L-positive cells is shown in the upper right corner of each panel. Mock iPS-T cells or CD4^{+} iPS-T cells were stimulated with PHA-P, cultured for 12 days in the presence of IL-7 and IL-15, and then cultured for 24 h in the presence of IL-2 and IL-15. **(B, C)** Expressions of CD40L, CD4, and TCR-Vβ9 on each subpopulation are shown. CD40L high and low populations were separated from Mock iPS-T cells or CD4^{+} iPS-T cells by flow cytometry sorting and expanded by PHA-P stimulation. **(D, E)** Surface CD40L expression on different subpopulations stimulated with plate-bound control IgG or anti-CD3 mAb (10 μg/mL). The original CD4^{+} Th clone (SA32.5) served as a control. Relative fluorescence intensity (RFI) is shown in the upper right corner of each panel. **(B–E)** CD40L (red) and isotype-matched controls (gray) are shown. **(F)** Representative flow cytometry profiles of the indicated molecules on DCs. Vehicle- or b3a2-peptide-pulsed DCs were cultured for 24 h with the indicated population at a DC/CD4^{+} iPS-T cell ratio of 5:1. OK432 (10 μg/mL)-matured DCs and medium-control

DCs served as controls. The indicated surface molecules (red) and isotype-matched controls (gray) are shown. **(G)** IL-10 production by DCs or B cells co-cultured with the indicated population. IL-10 in the culture supernatant was measured by ELISA. The indicated population (2×10^4) was co-cultured for 24 h with autologous DCs or B cells (5×10^4) that had been prepulsed with b3a2 peptide (10 μM). Data shown are the means ± SD of triplicate cultures and are representative of two independent experiments. **(H)** Representative flow cytometry profiles of the indicated molecules on K562 and THP-1.

Figure S8

Mechanism of the WT1-specific CTL priming via DC maturation by iPS-T cells, related to Figure 5

Mechanism of the WT1-specific CTL priming. b3a2, b3a2 peptide; pWT1, WT1 peptide. **(left panel)** When iPS-T cells recognize b3a2 peptide presented by DCs, the activated iPS-T cells up-regulate CD40L. **(center panel)** CD40 ligation by CD40L induces DC maturation. **(right panel)** Up-regulation of costimulatory molecules and enhanced cytokine production by DCs promote activation of WT1 peptide-specific CTLs.

Table S1

Antigen	Clone	Isotype
CD1a	HI149	mouse IgG1
CD3	OKT3	mouse IgG2a
CD3	UCHT1	mouse IgG1
CD4	OKT-4	mouse IgG2b
CD4	RPA-T4	mouse IgG1
CD5	UCHT2	mouse IgG1
CD7	CD7-6B7	mouse IgG2a
CD8 α	SK1	mouse IgG1
CD8 β	2ST8.5H7	mouse IgG2a
CD11c	MJ4-27G12	mouse IgG2b
CD14	M5E2	mouse IgG2a
CD19	HIB19	mouse IgG1
CD34	581	mouse IgG1
CD40	HB14	mouse IgG1
CD45	HI30	mouse IgG1
CD56	HCD56	mouse IgG1
CD80	2D10	mouse IgG1
CD83	HB15a	mouse IgG2b
CD86	IT2.2	mouse IgG2b
CD94	REA113	recombinant human IgG1
CD117 (c-Kit)	104D2D1	mouse IgG1
CD123	6H6	mouse IgG1
CD127	HIL-7R-M21	mouse IgG1
CD154 (CD40L)	24-31	mouse IgG1
CD161	HP-3G10	mouse IgG1
CD197 (CCR7)	G043H7	mouse IgG2a
CD226 (DNAM-1)	11A8	mouse IgG1
CD279 (PD-1)	EH12.2H7	mouse IgG1
CD294 (CRTh2)	BM16	rat IgG2a
CD303 (BDCA2)	AC144	mouse IgG1
CD314 (NKG2D)	1D11	mouse IgG1
CD335 (NKp46)	9E2	mouse IgG1
CD336 (NKp44)	P44-8	mouse IgG1
CD337 (NKp44)	P30-15	mouse IgG1
Fc ε R1	AER-37	mouse IgG2b
HLA-DR	L243	mouse IgG2a
TCR- α β	IP26	mouse IgG1
TCR- γ δ	B1.1	mouse IgG1
TCRBV9S1	FIN9	mouse IgG2a
TRBV22S1	IMMU546	mouse IgG1

Isotype control	Clone
mouse IgG1	MOPC-21
mouse IgG1	P3.6.2.8.1
mouse IgG2a	G155-178
mouse IgG2b	eBMG2b

Table S2

Pearson's correlation of gene expression between iPS-T cell samples and other cell types

Sample	Pearson correlation
iPS-Ts	0.962-0.974
NK	0.875-0.881
ILC1	0.884-0.891
ILC2	0.876-0.882
ILC3	0.868-0.871
α/β-T	0.845-0.853
γ/δ-T	0.876-0.882

Table S3

AHR	AREG	ASB2	BCL11B	CACNA1F	CCL5	CCL7	CCR3	CCR4	CCR5
CCR6	CCR7	CD226	CD3E	CEBPA	CEBPB	CHD7	CSF1	CSF2	CXCR3
CXCR6	EOMES	ETS1	ETS2	FASLG	FOSL1	FOXP3	GATA2	GATA3	GATA4
GFI1	GZMA	GZMB	GZMH	GZMK	GZMM	HAVCR2	HES1	HNF1A	HOPX
HOXA10	HOXA3	ICOS	ID2	ID3	IFNG	IFNGR1	IGSF6	IKZF1	IKZF2
IKZF3	IL10	IL12A	IL12B	IL12RB1	IL12RB2	IL13	IL13RA1	IL15RA	IL17A
IL17B	IL17C	IL17D	IL17F	IL17RB	IL17RE	IL18	IL18R1	IL18RAP	IL1R1
IL1R2	IL1RAP	IL1RL1	IL2	IL21	IL22	IL23R	IL2RA	IL2RB	IL2RG
IL4	IL4R	IL5	IL7R	IL9	IRF1	IRF4	IRF8	ITGAE	ITGB7
JAK1	KIF2C	KIT	KLRB1	KLRK1	LEF1	LRRC32	MAF	MYB	NCAM1
NCR1	NCR2	NCR3	NFATC1	NFATC2	NFIL3	NR4A1	NR4A3	PERP	PKD2
POU2F2	PPARG	PRF1	PTGDR2	RBPJ	REL	RELB	RORA	RORC	RUNX1
RUNX3	SATB1	SOCS1	SOCS5	SOX13	STAT1	STAT4	STAT5B	STAT6	TAL1
TBX21	TCF12	TCF7	TGIF1	THY1	TIGIT	TLR4	TLR6	TNF	TNFRSF9
TNFSF11	TOX	TP53INP1	UTS2	ZBTB16	ZBTB7B				

Table S4

Category	Term	Count	%	P-Value	Genes	List Total	Pop Hits	Pop Total	Fold Enrichment	Bonferroni
KEGG_PATHWAY	hsa04650:Natural killer cell mediated cytotoxicity	6	2.205882353	1.23E-05	PRF1, KLRK1, FASLG, GZMB, NFATC2, NCR1	14	133	5085	16.38560687	2.72E-04
KEGG_PATHWAY	hsa04630:Jak-STAT signaling pathway	5	1.838235294	4.79E-04	IL12RB2, IL2RB, STAT4, IL12RB1, JAK1	14	155	5085	11.71658986	0.01048484
KEGG_PATHWAY	hsa05330:Allograft rejection	3	1.102941176	0.003619614	PRF1, FASLG, GZMB	14	36	5085	30.26785714	0.076676827
KEGG_PATHWAY	hsa05332:Graft-versus-host disease	3	1.102941176	0.004238978	PRF1, FASLG, GZMB	14	39	5085	27.93956044	0.089221673
KEGG_PATHWAY	hsa04940:Type I diabetes mellitus	3	1.102941176	0.004904194	PRF1, FASLG, GZMB	14	42	5085	25.94387755	0.102513944
KEGG_PATHWAY	hsa05320:Autoimmune thyroid disease	3	1.102941176	0.007168701	PRF1, FASLG, GZMB	14	51	5085	21.36554622	0.146388778
KEGG_PATHWAY	hsa04060:Cytokine-cytokine receptor interaction	4	1.470588235	0.026326675	IL12RB2, IL2RB, IL12RB1, FASLG	14	262	5085	5.54525627	0.443977985

Table S5

Pearson correlation of gene expressions.

Cell samples		Pearson correlation
CD4 b3a2	Mock vehicle	0.934
	CD4 vehicle	0.945
	Mock b3a2	0.946
Mock vehicle	CD4 vehicle	0.956
	Mock b3a2	0.953
CD4 vehicle	Mock b3a2	0.948